JACS
JOURNAL OF THE AMERICAN CHEMICAL SOCIETY

Article

pubs.acs.org/JACS

Tetraalkylcuprates(III): Formation, Association, and Intrinsic Reactivity

Aliaksei Putau, Harald Brand, and Konrad Koszinowski*

Department Chemie, Ludwig-Maximilians-Universität München, Butenandtstrasse 5-13, 81377 München, Germany

Supporting Information

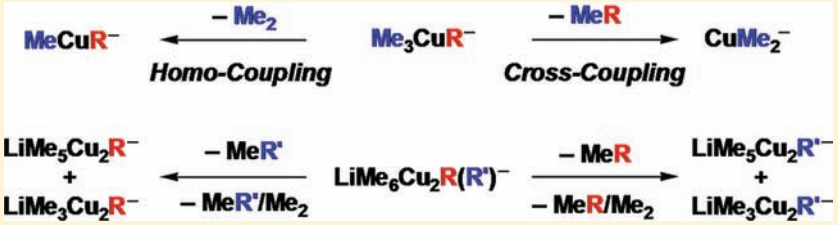

ABSTRACT: Tetraalkylcuprates are prototypical examples of organocopper(III) species, which remained elusive until their recent detection by NMR spectroscopy. In agreement with the NMR studies, the present electrospray ionization mass spectrometric experiments, as well as supporting electrical conductivity measurements, indicate that $LiCuMe_2 \cdot LiCN$ reacts with a series of alkyl halides RX. The resulting $Li^+Me_2CuR(CN)^-$ intermediates then afford the observable Me_3CuR^- tetraalkylcuprate anions upon Me/CN exchanges with added MeLi. In contrast, the reactions of $LiCuMe_2 \cdot LiCN$ with neopentyl iodide and various aryl halides give rise to halogen−copper exchanges. Concentration- and solvent-dependent studies suggest that lithium tetraalkylcuprates are not fully dissociated in ethereal solvents, but partly form $Li^+Me_3CuR^-$ contact ion pairs and presumably also triple ions $LiMe_6Cu_2R_2^-$. According to theoretical calculations, these triple ions consist of two square-planar Me_3CuR^- subunits binding to a central Li^+ ion. Upon fragmentation in the gas phase, the mass-selected Me_3CuR^- anions undergo reductive elimination, yielding both the cross-coupling products MeR and the homocoupling product Me_2. The branching between these two fragmentation channels markedly depends on the nature of the alkyl substituent R. The triple ions $LiMe_6Cu_2R_2^-$ (as well as their mixed analogues $LiMe_6Cu_2R(R')^-$) also afford both cross-coupling and homocoupling products upon fragmentation, but strongly favor the former. On the basis of theoretical calculations, we rationalize this prevalence of cross-coupling by the preferential interaction of the central Li^+ ion of the triple ions with two Me groups of each Me_3CuR^- subunit, which thereby effectively blocks the homocoupling channel. Our results thus show how a Li^+ counterion can alter the reactivity of an organocopper species at the molecular level.

1. INTRODUCTION

The late transition metal copper forms organometallic reagents of outstanding importance to organic synthesis.[1] Virtually all of these reagents correspond to Cu(I) species with a $3d^{10}$ valence electron configuration.[2,3] The reactions of organocopper(I) reagents with carbon electrophiles, such as alkyl halides, epoxides, and Michael acceptors, have long been postulated to involve Cu(III) intermediates,[4] which have also been predicted by theoretical calculations.[5] Because of their supposedly very high propensity toward reductive elimination, these organocopper(III) species were believed to be too elusive for detection.[4,6] Recently, however, Bertz, Ogle, and co-workers[7] as well as the Gschwind group[8] succeeded in observing several organocopper(III) compounds by low-temperature NMR spectroscopy. This breakthrough now opens the door to further investigations of Cu(III) species to complement our knowledge of organocopper chemistry. Besides being of fundamental importance, a better understanding of organocopper(III) compounds and their reactivity also promises practical benefits, as it might help in optimizing reagents and reaction conditions in a rational way. Among the organocopper(III) species so far identified, the tetraalkylcuprate anions are particularly interesting. These species have been observed in the course of cross-coupling reactions between lithium dimethylcuprate $LiCuMe_2 \cdot LiCN$ (**1**) and alkyl halides RX and in some cases even were found to survive warming to 20 °C for short times.[7b,e] This enhanced stability renders tetraalkylcuprates ideal model systems not only for studying the generation of organocopper(III) compounds but also for probing their reactions.

Here, we investigate the formation and reactivity of tetraalkylcuprate anions by a combination of different methods. Specifically, we use electrospray ionization mass spectrometry (ESI-MS)[9] to analyze the tetraalkylcuprate ions produced in the reactions of **1** and other diorganylcuprates with a series of alkyl halides; for comparison, we also sample the ionic products of the reactions of **1** with several aryl halides. ESI-MS is increasingly recognized as a valuable tool to characterize charged organometallics in general[10] and organocuprate anions in particular.[11,12] Unlike most other analytical techniques, it has the great advantage of affording unambiguous stoichiometric information. For selected cases, we complement the ESI-MS experiments by electrical conductivity measurements. In addition, we

Received: October 6, 2011
Published: November 30, 2011

   dx.doi.org/10.1021/ja209433j | J. Am. Chem.Soc. 2012, 134, 613−622

apply gas-phase methods to assess the unimolecular reactivity of mass-selected tetraalkylcuprate anions. Gas-phase studies have already proven valuable for probing the intrinsic reactivity of dialkylcuprates(I).[12a,13] To aid in the interpretation of the gas-phase experiments, we also perform quantum-chemical calculations.

2. EXPERIMENTAL AND THEORETICAL METHODS

2.1. Materials and General Methods. Standard Schlenk techniques were applied in all cases. Tetrahydrofuran (THF) was distilled from sodium/benzophenone. Cyclopentyl methyl ether and methyl *tert*-butyl ether were dried over molecular sieves (4 Å). CuCN was dried by repeated heating under a vacuum at 350 °C. Solutions of organolithium compounds RLi were used as purchased: MeLi (1.49 M) in Et_2O, EtLi (0.42 M) in benzene/cyclohexane (90/10), BuLi (2.37 M) in hexane, ^{t}BuLi (1.88 M) in pentane, and PhLi (1.74 M) in Bu_2O. The exact concentrations were determined by titration of 1,3-diphenyl-2-propanone tosylhydrazone.[14] For the labeling experiments, CD_3I (Sigma Aldrich, 99.5% D content), EtI-d_5 (Sigma Aldrich, 99.5% D content), and BuI-d_9 (Ehrenstorfer, 99.3% D content) were employed.

2.2. Sample Preparation. Sample solutions of $LiCuMe_2$·LiCN/RX stoichiometry were prepared by adding MeLi (2 equiv) to suspensions of CuCN in dry ethereal solvents at −78 °C and stirring at this temperature for 15 min to approximately 1 h before the organyl halide RX was added (1 equiv). Addition of further MeLi (1 equiv) afforded sample solutions of CuCN/3 MeLi/RX stoichiometry, which alternatively could be prepared by treatment of CuCN suspensions with 3 equiv of MeLi (−78 °C, 1 h), followed by the addition of RX (1 equiv). Analogous procedures provided solutions of $LiCuR'_2$·LiCN/RX.

2.3. Electrospray Ionization Mass Spectrometry. ESI of solutions of reactive organometallics in THF is challenging because of (i) the predominance of ion pairing in this relatively low-polarity solvent and the corresponding small concentration of free ions and (ii) the sensitivity of these reagents toward traces of moisture present in the inlet system. To mitigate these problems, relatively high sample concentrations of typically $c \approx 25$ mM were used, similarly to several previous studies.[12,15] Moreover, great care was taken to exclude moisture from the inlet system and to flush the system with dry solvent before injection of the sample solution. Aliquots of the sample solutions were administered into the ESI source of an HCT quadrupole ion trap (Bruker Daltonik) via a pump-driven gastight syringe at flow rates of 0.3−1.0 mL h^{-1}.

The ESI source was operated with N_2 as nebulizer gas (0.7 bar backing pressure) and drying gas (5 L min^{-1} flow rate, 60 °C) at an ESI voltage of −3 kV. The produced ions passed a capillary, a skimmer, and two transfer octopoles before entering the quadrupole ion trap. The voltages applied to these components were identical to those used previously[12] to ensure particularly mild conditions. The ion trap was filled with helium (estimated pressure $p(\mathrm{He}) \approx 2$ mTorr) and operated at a trap drive of 20 (the trap drive corresponds to the m/z value of the low-mass cutoff in the stability diagram of the ion trap). Mass spectra were recorded for m/z = 50−1000.

2.4. Gas-Phase Fragmentation Experiments. For the fragmentation experiments, the mass-selected ions (mass windows of 1−2 amu) were subjected to excitation voltages of amplitudes V_{exc} (peak-to-peak amplitudes, applied to one of the end-caps of the ion trap) for t = 40 ms and were simultaneously allowed to collide with the He gas. Note that the low-mass cutoff of the ion trap prohibits the detection of fragment ions, whose m/z ratio is ≤27% of that of the parent ion. The given branching ratios of the fragmentation reactions are the averages of different individual experiments/scans. The quoted uncertainties are based on the corresponding standard deviations and do not include any systematic errors, which are supposed to be negligible. In the case of the fragmentation of the $LiMe_6Cu_2R_2^-$ triple ions, the detection of $LiMe_3Cu_2(OH)^-$ pointed to a consecutive reaction of the $LiCu_2Me_4^-$ fragment ion with background water present in the ion trap, eq 1. In line with this rationalization, the amount of detected $LiMe_3Cu_2(OH)^-$ correlated

$$LiCu_2Me_4^- + H_2O \rightarrow LiCu_2Me_3(OH)^- + MeH \quad (1)$$

with the excitation time t (Supporting Information, Figures S52−S54). Experiments on mass-selected $CuMe_2^-$ and $LiCu_2Me_4^-$ produced by ESI of solutions of $LiCuMe_2$·LiCN in THF confirmed that only the latter readily undergoes efficient hydrolysis reactions under the experimental conditions applied. In the case of $LiMe_6Cu_2R_2^-$ (R = allyl) and its fragment ions, apparently additional consecutive hydrolysis reactions occur and complicate the analysis to such an extent that no branching ratios between cross-coupling and homocoupling reactions could be determined.

To investigate whether the excitation voltages V_{exc} could be converted into absolute energies in a straightforward manner,[16] we studied the fragmentation behavior of a series of benzylpyridinium ions (Figures S43 and S44); the activation energies associated with their dissociation had previously been derived from theoretical calculations.[17] Unlike Zins et al.,[16b] we did not find a satisfactory correlation between the obtained appearance voltages V_{appear} of the fragment ions (for the definition of V_{appear}, see Figure S43) and the calculated activation energies AE_{calc} reported in the literature (Figure S44).[16] Hence, a conversion of the V_{exc} values into absolute energies does not appear possible for the employed ion trap.

2.5. Electrical Conductivity Measurements. Electrical conductivity measurements were performed with a SevenMulti instrument (Mettler Toledo) and a stainless steel electrode cell (InLab741, Mettler Toledo, $\kappa_{cell} = 0.1$ cm^{-1}) calibrated against a 0.1 M solution of aqueous KCl at 298 K. Test measurements of solutions of $NaBPh_4$ in THF[18] showed that the instrument also worked correctly at low temperatures (Figure S1). Solutions of $LiCuMe_2$·LiCN in THF (of nominal concentration c = 100 mM) with and without added RCl (R = allyl) were analyzed at 202 K in order to slow down interfering hydrolysis reactions. Nonetheless, the latter were found to reduce the concentration of the active dimethylcuprate reagent by 20 ± 5% (as determined by iodometric titration).[19] The amount of hydrolysis thus exceeds that previously determined for $LiCuR_2$·LiCN solutions (R = Bu, ^{t}Bu, and Ph),[12b] which points to a particularly high sensitivity of the dimethylcuprate reagent.

2.6. Quantum-Chemical Calculations. Theoretical calculations were performed with the program package Gaussian 03.[20] All calculations refer to the gas phase, thus making possible a direct comparison with the gas-phase experiments. Similarly to related previous work,[8c,21] a first set of density functional theory (DFT) calculations employed the B3LYP hybrid functional[22] and an effective core potential with 10 core electrons for the Cu atoms (B3LYP/6-31G*/SDD).[23] As discussed below, the resulting activation energies for the fragmentation reactions of the Me_3CuR^- complexes appeared to be biased in favor of the homocoupling channel (see section 3.3.2). For the fragmentation of Me_3CuEt^-, we therefore performed exploratory calculations with other methods, including B3LYP/6-31G* all-electron calculations (Table S9).[24] With a larger basis set and the MDF effective core potential with 10 core electrons,[25] Møller−Plesset perturbation[26] theory (MP2/6-311+G*/MDF) exhibited a somewhat improved behavior at affordable costs (Table S9) and was used for further calculations on the mononuclear Me_3CuR^- anions and their unimolecular reactions. Vibrational analyses were performed to classify stationary points as local minima (zero imaginary frequencies) or transition states (one imaginary frequency). All energies given are zero-point corrected. Minimum energy structures were calculated for different coordination modes (for the triple ions $LiMe_6Cu_2R_2^-$), but the complete conformational space was not searched. Instead, staggered alkyl chain conformations were used as starting points for the geometry optimizations. For the case of $LiCu_2Me_8^-$, we not only performed B3LYP calculations (B3LYP/6-31G*/SDD), but also employed other functionals, such as the B3PW91[27] and MPW1PW91 functionals,[28] as well as Møller−Plesset perturbation theory to check the robustness of the predicted coordination geometry. The C−Li and Cu−Li interactions of the resulting optimized structures were also characterized by natural bond orbital

dx.doi.org/10.1021/ja209433j | J. Am. Chem.Soc. 2012, 134, 613−622

analyses (Table S21).[29] Moreover, for the allyl-containing cuprate ions Me_3CuR^- and $MeCuR^-$ (R = allyl), we considered not only σ-bound but also π-bound isomers. The latter were consistently found to be unstable. The DFT method also predicted the transition structure associated with the reductive elimination of MeR from Me_3CuR^- to correspond to a σ-bound complex. In contrast, our MP2 calculations did not find an analogous σ-bound transition structure, but only a π-bound isomer. To compute nonetheless at least an approximate activation energy for the MeR elimination with this method, we considered a transition structure with optimized geometry except for the distance between the β-C atom and the Cu center, which was held constant at 250 pm, i.e., the distance derived from the DFT calculations.

3. RESULTS AND DISCUSSION

3.1. Reactions of Dialkylcuprates with Organyl Halides.

3.1.1. Reactions of Dimethylcuprate with Alkyl Halides. Upon addition of 1 equiv of allyl chloride to a solution of **1** in THF, the electrical conductivity markedly decreases (Figures 1 and S2). At the same time, the ESI signal

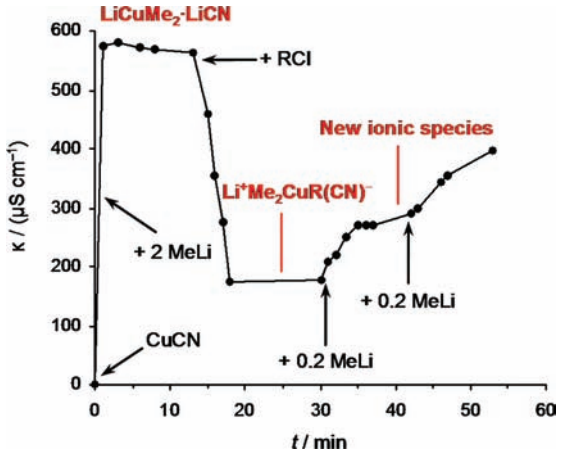

Figure 1. Time profile of the electrical conductivity of a solution of $LiCuMe_2$·LiCN (**1**) in THF (generated by the addition of 2 equiv of MeLi to CuCN) at 202 K upon consecutive treatment with RCl (R = allyl, 1 equiv) and MeLi (2 × 0.2 equiv).

intensities of the $Li_{n-1}Cu_nMe_{2n}^-$ ions characteristic of solutions of **1** in THF[12a] almost completely vanish. According to Bertz et al.,[7b] we rationalize this behavior by the generation of an $Li^+Me_2CuR(CN)^-$ intermediate (R = allyl). Due to its relatively low stability,[8c] the $Me_2CuR(CN)^-$ anion presumably does not survive the ESI process, thus explaining our inability to detect it by ESI-MS. If further MeLi is added, the conductivity slowly increases again, indicating the formation of a new ionic species (Figure 1). Similar results are obtained when CuCN/3 MeLi is treated with RCl (Figure S3). In this case, the conductivity first sharply drops but then slowly recovers as the transient $Li^+Me_2CuR(CN)^-$ reacts with excess MeLi present in solution to yield the ionic species already known from the previous experiment.

ESI-MS identifies the newly formed ionic species as the tetraalkylcuprate Me_3CuR^- (Figure 2), which apparently originates from $Li^+Me_2CuR(CN)^-$ via a methide/cyanide exchange (Scheme 1). In addition to mononuclear Me_3CuR^-, we also observe the corresponding triple ion, i.e., the Li^+-bound dimer $LiMe_6Cu_2R_2^-$. The aggregation equilibrium interrelating mononuclear tetraalkylcuprates and the related dimeric complexes will be discussed in detail in section 3.2.

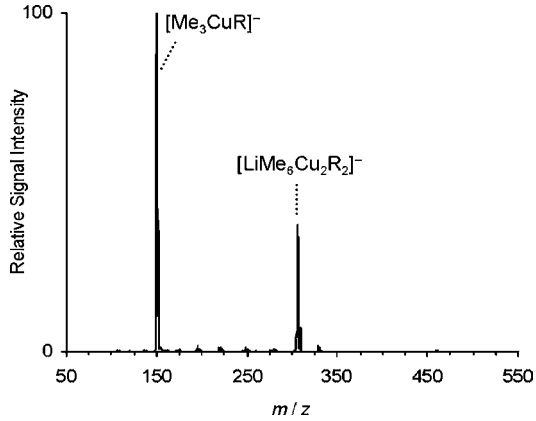

Figure 2. Negative ion mode ESI-MS of a solution of the products formed in the reaction of $LiCuMe_2$·LiCN (**1**) with RCl (R = allyl) in THF.

Scheme 1. Formation of Lithium Tetraalkylcuprates Li^+2a–g Probed by ESI-MS

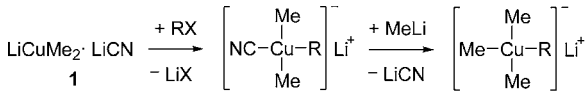

RX = MeI, EtI, PrI, BuI, $PhCH_2CH_2I$, $CH_2{=}CHCH_2Cl$, $CH_2{=}CHCH_2Br$, $CF_3CH_2CH_2I$

Li^+**2a**, R = Me
b, Et
c, Pr
d, Bu
e, CH_2CH_2Ph
f, $CH_2CH{=}CH_2$
g, $CH_2CH_2CF_3$

Analogous ESI-MS experiments demonstrate that **1** reacts not only with allyl chloride but also with MeI, EtI, PrI, BuI, $PhCH_2CH_2I$, and $CH_2{=}CHCH_2Br$ to yield tetraalkylcuprates Me_3CuR^- (**2a–f**) and $LiMe_6Cu_2R_2^-$ (**3a–f**, Scheme 1 and Figures S4–S8). Note that **2a**, **2b**, and **2f** are already known from NMR spectroscopic experiments,[7b,d–f,8a,c] whereas **2c–e** have not been reported before. The given assignments are based on observed m/z ratios, isotopic patterns, and, for selected systems, isotopic labeling experiments (Figures S9–S14). Additional and unambiguous evidence for the identities of the tetraalkycuprate ions comes from their fragmentation behavior (see section 3.3.1). Solutions of Li^+**2b–g** kept at room temperature are stable for approximately 1 h, after which time Cu(I) decomposition products containing CN^- and I^- start to appear. In the case of Li^+**2a**, such decomposition products are already observed immediately after sample preparation (Figure S4). The putative Cu(III) species formed upon reaction of **1** with $CH_2{=}CHCH_2I$ and BnBr (Bn = benzyl), respectively, prove to be even less stable and completely elude detection by ESI-MS. In contrast, PrCl, BnCl, PrBr, $(CH_3)_3CCH_2Br$, and ^{i}PrI do not react with **1** at all. From these findings, we can derive the following trends in reactivity: (i) Alkyl iodides react faster than the corresponding bromides (compare, e.g., PrI and PrBr), whereas the chlorides are even less reactive (compare, e.g., BnBr and BnCl). (ii) Primary alkyl halides react faster than secondary ones (compare, e.g., PrI and ^{i}PrI). This behavior matches that of typical S_N2 processes[30] and thus strongly suggests that the reaction of **1** with alkyl halides follows the same mechanism, in line with previous conclusions.[4a,Sd,7b]

dx.doi.org/10.1021/ja209433j | J. Am. Chem.Soc. 2012, 134, 613–622

A special situation is found for the reaction of **1** with 3,3,3-trifluoropropyl iodide. This reaction affords only small quantities of the expected tetraalkylcuprate **2g**, but mainly gives $Me_{4-n}CuR_n^-$ ions (R = $CF_3CH_2CH_2$ and n = 2–4) (Figure S15). We explain the formation of these species by the operation of iodine–copper exchange reactions between **1** and RI, leading to LiCu(Me)R·LiCN and $LiCuR_2$·LiCN reagents (Scheme 2), which can undergo sequential R/CN and R/Me

Scheme 2. Iodine–Copper Exchange Reactions Probed by ESI-MS

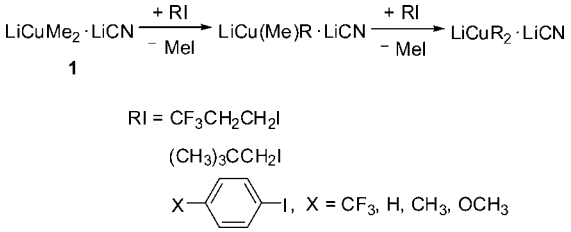

exchanges with the primary $Me_2CuR(CN)^-$ intermediate to yield the observed $Me_{4-n}CuR_n^-$ ions. Support for this rationalization is provided by the observation of $MeCuR^-$ and CuR_2^- (Figure S15). The increased tendency of $CF_3CH_2CH_2I$ to undergo iodine–copper exchange reactions obviously results from the electron-withdrawing effect of the terminal CF_3 group, which helps to stabilize the exchanged cuprates by a better delocalization of the negative charge. Interestingly, iodine–copper exchange also and exclusively occurs for the reaction of **1** with neopentyl iodide (Figure S16 and Scheme 2). Apparently, the iodine–copper exchange is less sensitive to steric constraints than an S_N2 reaction and therefore prevails over the latter for the relatively bulky neopentyl system.

3.1.2. Reactions of Dimethylcuprate with Aryl Halides. Analysis of mixtures of **1** and aryl iodides RI by negative ion mode ESI-MS shows the formation of R-bearing cuprates(I), $Li_{n-1}Cu_nMe_{2n-x}R_x^-$ (Figures 3 and S17–S20). These species

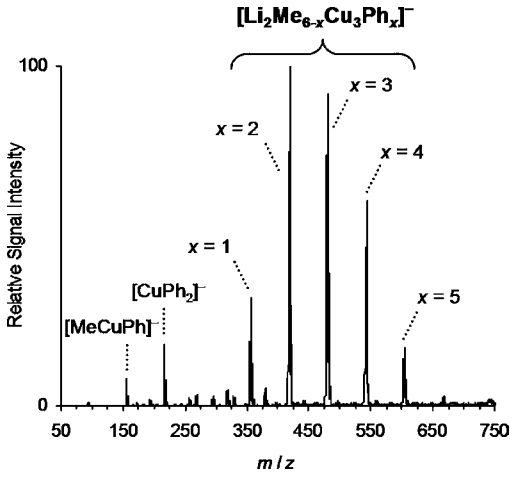

Figure 3. Negative ion mode ESI-MS of a solution of the products formed in the reaction of $LiCuMe_2$·LiCN (**1**) with PhI in THF.

originate from sequential iodine–copper exchange reactions (Scheme 2 for n = 1), which are well-known to occur upon treatment of dialkylcuprates with aryl halides.[4a,31] The driving force of these processes again is the better stabilization of the negative charge of the cuprate anions by the sp^2-hybridized and, thus, more electron-withdrawing carbon atoms of the aryl groups. The relative stability of the resulting aryl-containing cuprates can be further fine-tuned by changing their electronic properties: Acceptor-substituted *p*-trifluoromethylphenyl and simple phenyl groups enhance the stability, whereas donor-substituted *p*-tolyl and, in particular, *p*-anisyl groups reduce it, as can be seen from the higher propensity of the corresponding cuprates to degradation (Figures S18–S20).

We also investigated whether **1** undergoes halogen–copper exchange reactions with aryl bromides and chlorides as well. Mixtures of **1** and PhBr give ESI mass spectra essentially identical to those obtained for **1**/PhI. In contrast, **1** does not react with PhCl at room temperature. Similar reactivity orders are known for many other halogen–metal exchange reactions.[32]

3.1.3. Further Reactions of Dialkylcuprates with Organyl Halides. We also attempted to generate tetraalkylcuprates anions other than **2** (and the related triple ions **3**) and detect them by ESI-MS. The most obvious way to do so appears to be the reaction of diorganylcuprates $LiCuR_2$·LiCN (R ≠ Me) with alkyl halides R′X, which should afford $Li^+R_3CuR'^-$ species in analogy to the mechanism depicted in Scheme 1. In no case examined, however, was this approach successful (see Table S1). As an alternative method to prepare further tetraalkylcuprates, we started from **1** and treated it with BuI to generate a $Li^+Me_2CuBu(CN)^-$ intermediate as described above. Addition of 1 equiv of BuLi then yields $Me_2CuBu_2^-$ via a Bu/CN exchange, though apparently in rather small amounts. An analogous sequential treatment of **1** with PrI and BuLi affords $Me_2CuPr(Bu)^-$, but in even lower abundance than in the case of its $Me_2CuBu_2^-$ counterpart. A more efficient access to Cu(III) species containing three different alkyl substituents was found for the triple ions. Such $LiMe_6Cu_2R(R')^-$ complexes can be prepared by combination of **1** with 0.5 equiv of RI and 0.5 equiv of R′I (R/R′ = Et, Pr, Bu, $PhCH_2CH_2$, allyl; Figures S21–S26). A comparison of their relative abundances with those of the concomitantly formed $LiMe_6Cu_2R_2^-$ and $LiMe_6Cu_2R'_2^-$ species (i.e., **3**) shows an approximately statistical distribution and suggests that the reactions of **1** with the above-mentioned substrates occur at similar rates.

3.2. Association Equilibria of Lithium Tetraalkylcuprates. *3.2.1. Calculated Structures and Relative Energies in the Gas Phase.* Cu(III) species adopt $3d^8$ valence electron configurations, for which square-planar coordination geometries are energetically most favorable. Such square-planar geometries have indeed been found for tetraalkylcuprate anions,[7b,8a,c,21] and our theoretical calculations on **2a–f** (Figure S68) fully confirm this result. The gas-phase calculations moreover suggest that the triple ions **3** contain two subunits of intact **2**, which each interact with Li^+ via two of their methyl groups to form a distorted tetrahedral coordination environment (4-Me coordination of Li^+, Figures 4 and S73–S77; for the case of **3a**,

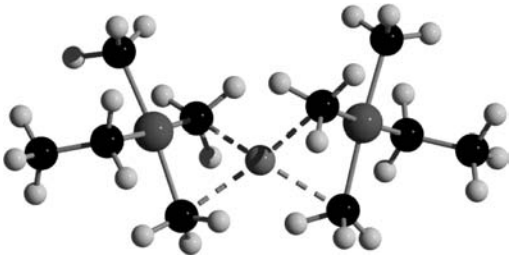

Figure 4. Calculated minimum energy structure of **3b** in the gas phase (gray, Cu; light gray, Li; black, C; white, H; B3LYP/6-31G*/SDD).

dx.doi.org/10.1021/ja209433j | J. Am. Chem.Soc. 2012, 134, 613–622

test calculations with various theoretical methods consistently found similar coordination geometries, see section 2.6 for details). In contrast, involvement of the R groups in the Li^+ coordination is predicted to be energetically slightly less favorable (Figures S73−S77 and Tables 1 and S16−S20). This difference presumably results from the smaller size of the methyl substituents, which permits their closer approach to the Li^+ center (Table 1) and thereby enhances the electrostatic interaction. The preferential interaction of Li^+ with methyl groups has also been inferred from a recent experimental study on cuprates(I).[12a]

Besides binding to the methyl groups, the Li^+ center may possibly also interact with the Cu atoms, given that the calculated Li−Cu distances are relatively short (Table 1) and that other d^8 systems, such as Pt(II),[33] have been shown to coordinate to Lewis acids via their d_{z^2} orbital. Presumably, the higher oxidation state of the Cu(III) atom substantially decreases the Lewis-basic character of its d_{z^2} orbital, however. In line with this argument, natural bond orbital analyses of the optimized structures of **3a** consistently find only rather weak Cu−Li interactions (see section 2.6 and Table S21).

For the case of **3a**, we also calculated its dissociation energy according to eq 2 with R = Me. In the gas phase, this

$$LiMe_6Cu_2R_2^- \rightarrow Me_3CuR^- + LiMe_3CuR \quad (2)$$

reaction is highly endothermic ($\Delta_{react}E$ = 165 kJ mol^{-1}). In solution, however, the situation most likely will be different because the release of the $LiMe_3CuR$ moiety should be facilitated by solvation.

3.2.2. Concentration- and Solvent-Dependent ESI-MS Measurements. The formation of triple ions AB_2^- from contact ion pairs A^+B^- and free ions B^- in solution is a well-known phenomenon.[34] Recently, ESI-MS has emerged as a valuable tool to characterize these species[35] and to study ion association in general.[12,37d] Accordingly, we have performed concentration- and solvent-dependent measurements of mixtures of **1** and allyl choride RCl (CuCN/3 MeLi/RCl) to

$$Li^+(solv) + 2Me_3CuR^- \rightleftharpoons Li^+Me_3CuR^-(solv) + Me_3CuR^- \rightleftharpoons LiMe_6Cu_2R_2^- \quad (3)$$

gain further insight into the association equilibria leading to the formation of **3f**, eq 3.

With increasing concentration of CuCN/3 MeLi/RCl in THF, the relative ESI signal intensity of **2f** strongly decreases, whereas that of the triple ion **3f** rises correspondingly (Figure 5).

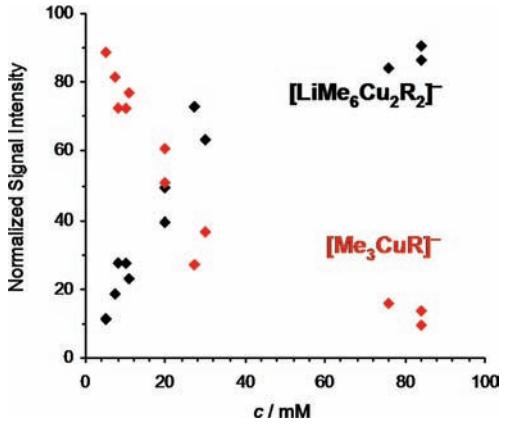

Figure 5. Normalized ESI signal intensities of Me_3CuR^- (red) and of the corresponding triple ion $LiMe_6Cu_2R_2^-$ (black, R = allyl) as functions of the concentration *c* of CuCN/3 MeLi/RCl in THF.

This trend matches the behavior expected on the basis of the law of mass action, which predicts a shift toward higher aggregation states as a function of concentration (eq 3).

For assessing the effect of the solvent, we also probed mixtures of CuCN/3 MeLi/RCl in cyclopentyl methyl ether and methyl *tert*-butyl ether. Cu(III) species are not observed for reaction assays in the pure solvents (Figures S27 and S28), but only for solutions of Li^+**2f**/**3f** prepared by preformation in THF and further dilution (Figures S29 and S30). In the case of the cyclopentyl methyl ether/THF mixtures, the observed fraction of monomeric **2f** is slightly decreased in comparison to the situation in pure THF (Table S2). This finding can be rationalized by the lower polarity and smaller Li^+ affinity of cyclopentyl methyl ether, which make solvation less favorable and thus shift the equilibrium toward contact ion pairs and higher aggregation states (eq 3). For mixtures of the even less polar methyl *tert*-butyl ether with THF, one would expect a somewhat stronger effect, whereas just the opposite holds true (Table S2). Possibly, the interaction of methyl *tert*-butyl ether molecules with the lithium cuprates-(III) is so weak that they are displaced by THF molecules, thus giving rise to a local environment similar to that in pure THF solutions.

According to our measurements, all probed lithium tetraalkylcuprates Li^+**2** have roughly similar tendencies to form the corresponding triple ions **3**. With ESI-MS, we cannot determine the absolute equilibrium concentrations of **3** in THF solutions, however, because the detected analyte ions do not stem directly from the sampled solution, but rather from charged nanodroplets generated in the course of the ESI process.[36] Previous studies have shown that the analyte

Table 1. Relative Energies (in kJ mol^{-1}) as Well as Li−C and Li−Cu Bond Distances (in pm) of the Different Isomers of 3a−f According to B3LYP/6-31G*/SDD Calculations

	4Me coordination of Li^+			3Me−R coordination of Li^+				2Me−2R coordination of Li^+			
	E_{rel}	$r(Li-C_{Me})^a$	$r(Li-Cu)^a$	E_{rel}	$r(Li-C_{Me})^a$	$r(Li-C_R)$	$r(Li-Cu)^a$	E_{rel}	$r(Li-C_{Me})^a$	$r(Li-C_R)^a$	$r(Li-Cu)^a$
3a	0	225	250								
3b	0	224	251	6.4	224	231	249	12.1	224	234	247
3c	0	224	252	5.5	224	232	249	11.8	223	234	247
3d	0	224	251	5.7	224	233	248	11.6	223	234	248
3e	0	223	251	8.3	223	234	249	15.9	222	235	247
3f	0	223	251	7.0	223	233	249	15.8	221	238	247

[a]Values given refer to the average of the different individual bond lengths.

dx.doi.org/10.1021/ja209433j | J. Am. Chem.Soc. 2012, 134, 613−622

concentration in these nanodroplets is higher than in the sampled solutions[37] and that their effective temperature may also change.[38] In the sampled solutions, in turn, the concentration of the triple ions **3** may be too low for their detection by NMR spectroscopy. Moreover, the interconversion between **2** and **3** could occur faster than the NMR time scale, which might be another reason why no triple ions **3** have been observed by this method.

3.2.3. Electrical Conductivity Studies. The molar electrical conductivity of **1** in THF is similar to those of the related lithium diorganylcuprates $LiCuR'_2{\cdot}LiCN$ (R′ = Bu, ^{t}Bu, and Ph).[12b] On the basis of a comparison of the measured conductivities with their estimated limiting conductivities, we have suggested that these reagents are not fully dissociated in THF, but partly form contact ion pairs.[12b] A similar situation can also be inferred for **1**. Upon the addition of 1 equiv of allyl chloride and the formation of the $Li^+Me_2CuR(CN)^-$ intermediate (R = allyl), the electrical conductivity significantly decreases (Figure 1). This decrease points to a lower dissociation tendency of $Li^+Me_2CuR(CN)^-$. Lithium cuprates(I) that contain cyanide ligands attached to the copper exhibit an analogous behavior, which we have ascribed to the ambident nature of the cyanide ion and its ability to coordinate to copper and lithium centers simultaneously.[12b] The electrical conductivity of Li^+**2f** is higher again and roughly equals that of **1** (Figures 1 and S3), indicating a similar equilibrium between solvent-separated and contact ion pairs. The presence of the latter is a prerequisite for the formation of **3** according to eq 3.

3.3. Unimolecular Reactivity of Tetraalkylcuprates. *3.3.1. Fragmentation of Mononuclear Tetraalkylcuprate Anions.* In the final step in the generally accepted mechanism of copper-mediated cross-coupling reactions, the Cu(III) intermediate releases the coupling product in a reductive elimination. Gas-phase experiments on tetraalkylcuprates as Cu(III) model systems offer the possibility to study this important elementary reaction in great detail. For mass-selected **2a**, the collision-induced dissociation (CID), as expected, leads to the formation of $CuMe_2^-$ and the concomitant elimination of ethane (Figure S31). Analogous experiments with labeled $Me_3CuCD_3^-$ determine the secondary kinetic isotope effect of this reaction as KIE = 1.0 ± 0.1 (determined for an excitation voltage of V_{exc} = 0.33 V). For the other, unsymmetrical tetraalkylcuprate anions **2b**–**g**, two different fragmentation channels are available: elimination of the cross-coupling product MeR or of the homocoupling product ethane, eqs 4 and 5, respectively (Figures 6 and S32–S38). If the homocoupling $MeCuR^-$ fragment ions contain β-hydrogen atoms, β-H eliminations can ensue and lead to $MeCuH^-$ secondary fragment ions, as has been shown previously.[12a,13d]

$$Me_3CuR^- \rightarrow CuMe_2^- + MeR \quad (4)$$

$$\rightarrow MeCuR^- + Me_2 \quad (5)$$

For a comparison of the competition between cross-coupling and homocoupling reactions of the tetraalkylcuprates **2b**–**g**, we first consider relatively harsh CID conditions (V_{exc} = 0.25–0.30 V), resulting in the fragmentation of >70% of the parent ion population (Figures S32–S38). Whereas **2b** and **2c** preferentially afford the cross-coupling product, **2d** gives a 1:1 fragment ratio, which corresponds to a purely statistical branching; in contrast, **2e**–**g** mainly yield the homocoupling product (Table 2). We can also compare the fragmentation pattern of **2g** with that of the related $Me_{4-n}CuR_n^-$ ions, R = $CF_3CH_2CH_2$ and n = 2–4 (Figures S39–S41). As expected, CuR_4^- only releases R_2, while $MeCuR_3^-$ exclusively eliminates MeR; $Me_2CuR_2^-$, in turn, loses MeR and Me_2 in approximately equal amounts (Table S3). The latter case is particularly interesting because $Me_2CuR_2^-$ can form two different isomers. For the *trans*-isomer, cross-coupling reactions should be strongly preferred, whereas the *cis*-isomer could yield both cross-coupling and homocoupling products. The observed branching ratio suggests that the *cis*-isomer is at least partly present. Furthermore, the $CF_3CH_2CH_2$ group apparently has an intrinsically lower tendency to participate in the reductive elimination than methyl. For the related $Me_2CuBu_2^-$ anion, the simultaneous occurrence of cross-coupling and homocoupling reactions (losses of Bu_2 and Me_2) also points to the partial presence of the *cis*-isomer (Figure S42 and Table S3).

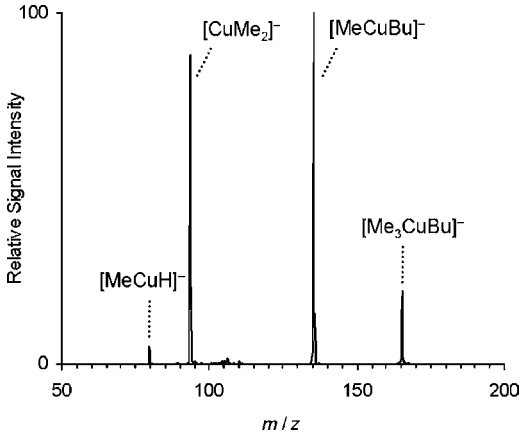

Figure 6. Mass spectrum of mass-selected **2d** (m/z = 165) and its fragment ions produced upon collision-induced dissociation (V_{exc} = 0.23 V).

Upon variation of the excitation voltage V_{exc}, and, thus, the effective temperature of the parent ions **2a**–**f**, the branching ratios between cross-coupling and homocoupling reactions remain largely unchanged (Figures S45–S49). Moreover, the determined appearance voltages V_{appear} for the fragmentations, corresponding to very approximate relative threshold energies (see Figure S43 for technical details), show a similar trend: The cross-coupling channel is energetically slightly favored for **2b**–**d**, whereas the homocoupling channel is energetically more favorable for **2e** and **2f** (Table 2). This consistency indicates that the observed branching ratios reflect the true intrinsic behavior of the tetraalkylcuprate anions. Accordingly, a comparison of the present gas-phase data with solution-phase results from the literature appears meaningful.

In solution, reactions of **1** with simple aliphatic alkyl halides give the synthetically desired cross-coupling products in high yields,[4a] whereas increased amounts of homocoupling were reported for a few reactions involving diallyl-[39] and dihexylcuprates.[40] In their theoretical analysis of the competition between cross-coupling and homocoupling, Bäckvall, Nakamura, and co-workers focused on the coordination geometry of the neutral R'_2CuR intermediates for explaining the usually observed preference for cross-coupling reactions.[40] The present results suggest that different organyl substituents may also have intrinsically different tendencies toward cross-coupling or homocoupling, respectively.

3.3.2. Calculated Fragmentation Pathways of Mononuclear Tetraalkylcuprate Anions. Theory predicts high

dx.doi.org/10.1021/ja209433j | J. Am. Chem.Soc. 2012, 134, 613–622

Table 2. Branching Fractions and Appearance Voltages V_{appear} (in Volts, as Approximate Measures for Relative Threshold Energies) of the Fragmentation Reactions of Tetraalkylcuprate Anions 2

	cross-coupling (eq 4)		homocoupling (eq 5)	
Me_3CuR^- (R)	fraction[a]	V_{appear}	fraction[a]	V_{appear}
2a (Me)	0		1	
2b (Et)	0.93 ± 0.01	0.201 ± 0.001	0.07 ± 0.01	0.205 ± 0.005
2c (Pr)	0.61 ± 0.04	0.214 ± 0.002	0.39 ± 0.04	0.215 ± 0.003
2d (Bu)	0.50 ± 0.05	0.180 ± 0.002	0.50 ± 0.05	0.183 ± 0.002
2e (CH_2CH_2Ph)	0.06 ± 0.01	0.196 ± 0.005	0.94 ± 0.01	0.192 ± 0.001
2f ($CH_2CH{=}CH_2$)	0.21 ± 0.02	0.199 ± 0.003	0.79 ± 0.02	0.186 ± 0.002
2g ($CH_2CH_2CF_3$)	0.00 ± 0.00		1.00 ± 0.00	

[a]Determined for V_{exc} = 0.30 V.

Table 3. Calculated Reaction and Activation Energies (in kJ mol^{-1}) of the Fragmentation Reactions of Tetraalkylcuprate Anions 2

	cross-coupling (eq 4)				homocoupling (eq 5)			
	$\Delta_{react}E$		$\Delta_{act}E$		$\Delta_{react}E$		$\Delta_{act}E$	
Me_3CuR^- (R)	DFT[a]	MP2[b]	DFT[a]	MP2[b]	DFT[a]	MP2[b]	DFT[a]	MP2[b]
2a (Me)					−174.1	−147.4	139.6	120.9
2b (Et)	−181.2	−149.6	148.9	131.1	−167.9	−130.1	141.4	131.4
2c (Pr)	−177.4	−142.1	152.6	134.6	−170.2	−131.7	138.7	128.7
2d (Bu)	−177.7	−139.7	152.9	134.8	−170.9	−131.7	138.3	128.7
2e (CH_2CH_2Ph)	−173.2	−122.3	153.2	136.4	−172.5	−132.0	134.9	126.1
2f ($CH_2CH{=}CH_2$)	−144.0	−104.8	150.9	143.8[c]	−177.4	−132.1	118.0	109.7

[a]B3LYP/6-31G*/SDD. [b]MP2/6-311+G*/MDF. [c]Calculated for a geometry with the distance between the β-C atom of the allyl substituent and the Cu center held constant at 250 pm; see section 2.6 for details.

exothermicities for the fragmentation reactions of tetraalkylcuprate anions **2**, pointing to the low thermodynamic stability of the Cu(III) species (Tables 3 and S4−S6; for calculated structures of the fragments, see Figures S69 and S70). Although DFT (B3LYP/6-31G*/SDD) and MP2 calculations with a larger basis set (MP2/6-311+G*/MDF) give considerably deviating *absolute* $\Delta_{react}E$ values, they find similar trends for the two competing fragmentation channels. While the cross-coupling reaction is significantly more exothermic than the homocoupling reaction for **2b** and moderately more exothermic for **2c** and **2d**, **2e** is a borderline case: the B3LYP calculations find a slightly larger exothermicity for the cross-coupling channel, whereas the MP2 calculations predict the homocoupling reaction to be more exothermic. In contrast, both theoretical methods agree that the cross-coupling reaction is much less exothermic for **2f**. This reduced exothermicity can be largely ascribed to the weakness of the newly formed C−C bond in the cross-coupling product 1-butene (compared to the C−C bonds in saturated *n*-alkanes, such as the homocoupling product Me_2 or the cross-coupling products formed from **2b−d**, see Table S22).

The theoretical activation energies $\Delta_{act}E$ display a parallel trend in that the relative preference for the homocoupling reaction increases in the series **2b−f** (Tables 3, S7, and S8). Whereas the DFT calculations in all cases find a lower energy barrier for the homocoupling reaction, the MP2 calculations with the larger basis set give more balanced barriers for both fragmentation channels. A comparison with the experimental V_{appear} values suggests that the calculations predict the correct trend for the activation barriers of the tetraalkylcuprates **2b−f**, but that they are biased in favor of the homocoupling reaction. Free activation energies $\Delta_{act}G$ computed for a large temperature range of 298 ≤ *T* ≤ 1000 K do not vary significantly, which is in agreement with the small temperature sensitivity found experimentally (Tables S10−S15).

The calculated activation energies for the reductive elimination of the tetraalkylcuprates **2** are much larger than those for neutral trialkylcopper(III) species,[5d,6] for which values of 20 ≤ E_{act} ≤ 85 kJ mol^{-1} have been predicted.[41,42] Of course, the higher kinetic stabilities of the former are a prerequisite for their successful detection in the present experiments. To understand the reason for the stabilization of the tetraalkylcuprate anions **2** at a qualitative level, we compare the effect of attaching a methide ion to $CuMe_3$(III) versus CuMe(I). In the case of the highly electron-deficient and Lewis-acidic copper(III) species $CuMe_3$, a large stabilization should result (Scheme 3).

Scheme 3. Schematic Potential Energy Surfaces for the Reductive Elimination of Me_2 from Neutral $CuMe_3$ and Anionic $CuMe_4^-$

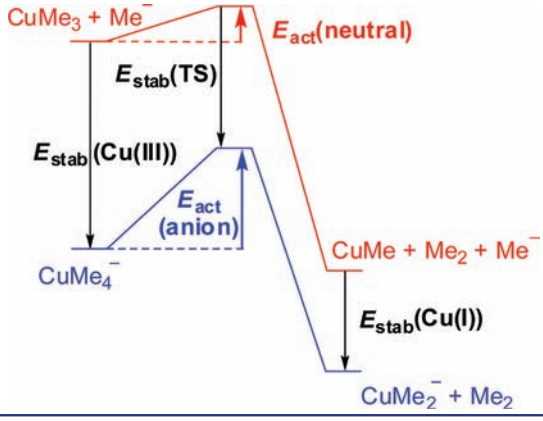

In contrast, the stabilization gained for CuMe is supposed to be much smaller. For the transition structure associated with the reductive elimination of Me_2, we expect an intermediate

dx.doi.org/10.1021/ja209433j | J. Am. Chem.Soc. 2012, 134, 613−622

behavior, which corresponds to the inferred increased activation energy for the anionic copper(III) species.

The reductive elimination of Me_2 from **2a** can also be compared with the analogous reaction of Me_3CuCl^-, which Pratt et al. have recently studied theoretically.[43] Both reactions exhibit similar transition structures of distorted tetrahedral geometries (see Figure 7 for the reductive elimination of Me_2

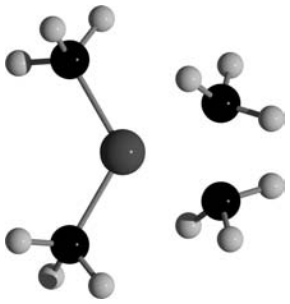

Figure 7. Calculated transition structure for the reductive elimination of Me_2 from **2a** (gray, Cu; black, C; white, H; B3LYP/6-31G*/SDD).

from **2a**; for reductive eliminations from **2b–f**, see Figures S71 and S72). However, the activation energy for the reductive elimination of Me_2 from **2a** is significantly higher. Presumably, this difference reflects the better stabilization of the Cu(III) center by a methide compared to that by a chloride ion (see above).

3.3.3. Fragmentation of $LiMe_6Cu_2R_2^-$ and $LiMe_6Cu_2R(R')^-$ Anions. The triple ions **3** form model systems that offer the possibility to assess the effect of a Li^+ counterion (paired with **2**) on the reactivity of the tetraalkylcuprates at a strictly molecular level. Like their monomeric counterparts **2**, the dimeric complexes **3** afford cross-coupling and homocoupling reactions upon CID, eqs 6 and 7, respectively (Figures S50–S60). The resulting mixed cuprate(I/III) fragment ions easily undergo consecutive reductive eliminations to form $LiCu_2Me_4^-$. The latter is partly hydrolyzed by a reaction with background water present in the ion trap, as we confirmed by control experiments (see Experimental and Theoretical Methods and Figures S52–S54).

$$LiMe_6Cu_2R_2^- \rightarrow LiMe_5Cu_2R^- + MeR \quad (6)$$

$$\rightarrow LiMe_4Cu_2R_2^- + Me_2 \quad (7)$$

We do not observe the elimination of any R_2 homocoupling products. Although their formation is clearly disfavored on simple statistical grounds, this argument appears insufficient to explain the complete absence of these reactions. Instead, we interpret this absence as another indication of **3** being composed of two separate subunits **2**, in line with our theoretical calculations (see section 3.2.1).

Compared to the monomeric tetraalkylcuprates **2**, the presence of the additional Li^+**2** subunit in **3b–e** substantially enhances the fraction of the cross-coupling (Table 4). We rationalize this difference by the preferential interaction of the Li^+ ion with the methyl groups in **3** (see section 3.2.1). With the four central methyl groups thus tied up, only the terminal Me and R substituents of **3** are supposedly prone to reductive elimination, thereby yielding the cross-coupling products. A deviating behavior is observed for **3f**·THF, which forms a rare example of an anionic THF complex sufficiently stable to survive the ESI process (detected for cyclopentyl methyl ether/

Table 4. Branching Fractions of the Fragmentation Reactions of the Triple Ions 3[a,b]

$LiMe_6Cu_2R_2^-$ (R)	fraction of cross-coupling (eq 6)	fraction of homocoupling (eq 7)
3b (Et)	0.93 ± 0.03	0.00 ± 0.00
3c (Pr)	0.91 ± 0.02	0.00 ± 0.01
3d (Bu)	0.86 ± 0.05	0.00 ± 0.00
3e (CH_2CH_2Ph)	0.54 ± 0.04	0.10 ± 0.04
3f·THF ($CH_2CH{=}CH_2$)	0.07 ± 0.03[c]	0.56 ± 0.03[c]

[a]The given fractions do not add up to 1 because of the presence of fragment ions, such as $Cu_2Me_3^-$ and $LiMe_3Cu_2R^-$, which cannot be unambiguously assigned to cross-coupling or homocoupling as primary fragmentation reaction, respectively. [b]Determined for V_{exc} = 0.30 V. [c]Determined for V_{exc} = 0.22 V.

THF mixtures, Figure S29). Possibly, the presence of the solvent molecule in **3f**·THF changes the coordination geometry of its $LiMe_6Cu_2R_2^-$ core in such a way that it no longer favors the cross-coupling channel (Table 4 and Figure S61).

Fragmentation experiments on *mixed* triple ions $LiMe_6Cu_2R(R')^-$ (Figures S62–S67) moreover make possible a direct comparison of different substituents R/R′ in their tendency to undergo reductive elimination. Such a comparison is particularly straightforward because the presence of the two R/R′ groups in the same parent ion ensures the availability of equal amounts of energy for both fragmentation pathways. The measured branching ratios consistently point to a clear order in the intrinsic reactivity of the different organyl substituents (Figure 8), which also largely agrees with the trends inferred

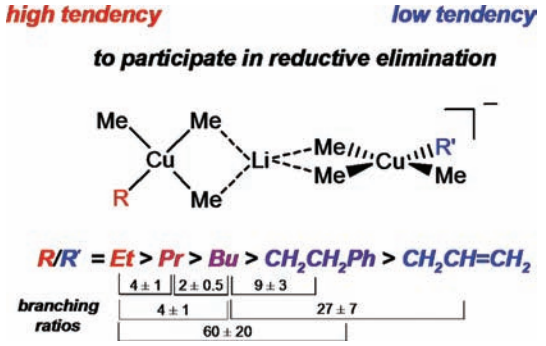

Figure 8. Tendencies of different R/R′ groups toward reductive elimination, as determined from the fragmentation of mixed triple ions $LiMe_6Cu_2R(R')^-$. The given branching ratios (listed at the bottom) not only are based on the observed signal intensities of the primary fragment ions (corresponding to losses of MeR and MeR′, respectively) but also take into account secondary fragmentation channels (losses of MeR/Me_2 and MeR′/Me_2, respectively).

from the fragmentation experiments on the mononuclear species **2b–f** (the fact that for the latter the homocoupling fraction observed for **2e** exceeds that for **2f** seems to be an anomaly; note that the appearance voltages V_{appear} derived for the homocoupling reactions of both species show the reversed order and are thus consistent with the behavior of the mixed triple ions).

3.3.4. Calculated Fragmentation Pathways of $LiCu_2Me_8^-$ and $LiCu_2Me_6^-$ Anions. DFT calculations (B3LYP/6-31G*/SDD) show that the reductive elimination of Me_2 from **3a** ($\Delta_{react}E$ = −186.9 kJ mol^{-1}) is more exothermic and has a smaller energy barrier ($\Delta_{act}E$ = 97.2 kJ mol^{-1}) than the analogous reaction of **2a** (Table 3). Presumably, the central Li^+

dx.doi.org/10.1021/ja209433j | J. Am. Chem.Soc. 2012, 134, 613–622

ion weakens the Lewis basicity of the attached methyl groups and, thus, reduces their stabilizing effect on the Cu(III) centers (see above); analogous behavior may also be expected for the other **3** anions. Note that the calculated fragmentation pathway involves two *terminal* methyl groups (Figure 9), in line with our

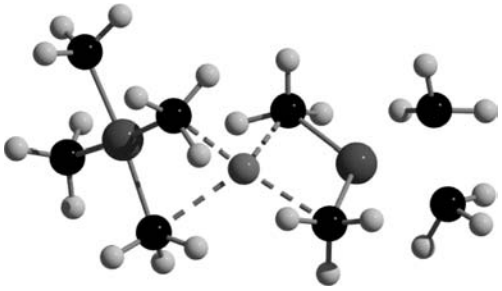

Figure 9. Calculated transition structure for the reductive elimination of Me_2 from **3a** (gray, Cu; light gray, Li; black, C; white, H; B3LYP/6-31G*/SDD).

qualitative arguments raised above (section 3.3.3). The resulting primary fragment ion $LiCu_2Me_6^-$ consists of a square-planar $CuMe_4^-$ and a linear $CuMe_2^-$ subunit, which coordinates to the central Li^+ ion via a single methyl group (Figure S78). The consecutive reductive elimination of Me_2 from $LiCu_2Me_6^-$ ($\Delta_{react}E$ = −181.2, $\Delta_{act}E$ = 96.6 kJ mol^{-1}) yields the complex $LiCu_2Me_4^-$, which contains two linear $CuMe_2^-$ subunits (Figure S78).

4. CONCLUSIONS

We have used electrospray ionization mass spectrometry to study the reactions of lithium dialkylcuprates $LiCuR'_2$·LiCN with organyl halides. At room temperature, only the dimethylcuprate **1** reacts with alkyl halides RX to afford observable copper(III) species. This enhanced reactivity of **1** is consistent with its wide use in organic synthesis. The reactivity pattern observed (reactivity decrease in the order RI > RBr > RCl and ^{prim}RI > ^{sec}RI) suggests that these reactions follow an S_N2 mechanism, in line with previous assumptions. If thermodynamically favored, halogen−copper exchange reactions can occur as well; for example, such exchange processes are observed upon reaction of **1** with aryl halides and neopentyl iodide or of $LiCuBu_2$·LiCN with MeI.

Electrical conductivity measurements indicate that the $Li^+Me_2CuR(CN)^-$ intermediates initially generated upon reaction of **1** with RX tend to form contact ion pairs in THF (R = allyl). A similar behavior has been noted for cyanide-containing cuprates(I) and was rationalized by the ambident nature of the cyanide ligand, which supposedly permits bridging binding modes between copper and lithium centers. Upon treatment with MeLi, the $Li^+Me_2CuR(CN)^-$ intermediates undergo a Me/CN exchange to yield the tetraalkylcuprates $Li^+Me_3CuR^-$ (Li^+**2**). These tetraalkylcuprates yield far more solvent-separated ion pairs than the $Li^+Me_2CuR(CN)^-$ intermediates, but are apparently still not completely dissociated in THF. Concentration- and solvent-dependent ESI-MS experiments also point to the operation of association equilibria in that they detect the triple ions $LiMe_6Cu_2R_2^-$ (**3**). These experiments cannot quantify the concentrations of the triple ions in the sampled solutions, however. The so-far lacking NMR spectroscopic evidence for their presence indicates that their concentrations must actually be rather small.

Whereas the reduced stability of organocopper(III) compounds and the operation of complex association equilibria severely impede reactivity studies in solution, the gas phase provides an ideal environment to probe the reactions of mass-selected tetraalkylcuprate ions. Upon fragmentation, both the mononuclear tetraalkylcuprates **2** and the triple ions **3** (as well as their mixed analogues $LiMe_6Cu_2R(R')^-$) undergo reductive elimination to yield cross-coupling and homocoupling products. The branching between the two fragmentation channels depends on the nature of the organyl substituent R, with the fraction of cross-coupling decreasing in the order R = Et > Pr > Bu > $PhCH_2CH_2$ ≈ CH_2=$CHCH_2$ (for a range of different collision energies and, thus, different effective temperatures). The branching ratios observed for the fragmentation of **3** are significantly shifted toward the cross-coupling, however. We explain this behavior by the action of the Li^+ ion present in **3**. According to our theoretical calculations, the triple ions **3** consist of two Me_3CuR^- subunits, which each bind to the central Li^+ ion with two of their Me groups. Tied up by this interaction with the lithium, these Me groups no longer readily participate in the reductive elimination, thereby suppressing the homocoupling channel. As is the case in organocopper(I) chemistry, the presence of Li^+ apparently can significantly change the course of reaction.

Our experiments clearly demonstrate the appreciable stability of tetraalkylcuprates(III). In comparison to neutral organocopper(III) species, this stability results from the addition of a strongly Lewis-basic Me^- or R^- anion to the highly electron-deficient Cu(III) center. While so far almost exclusively neutral organocopper(III) species have been considered as intermediates in copper-mediated cross-coupling reactions, the present experiments suggest that the participation of tetraalkylcuprate anions should also be taken into account if the overall reagent stoichiometry allows their formation (3 equiv of Me/R anions per Cu atom). This finding opens exciting prospects for further harnessing the unique reactivity of Cu(III) in organic synthesis.

■ ASSOCIATED CONTENT

Supporting Information

Additional electrical conductivity data, ESI mass spectra and data, and fragmentation mass spectra; results of energy-dependent fragmentation experiments; energies, structures, and bond orders obtained from quantum-chemical calculations; thermochemical data taken from the literature; and complete ref 20. This material is available free of charge via the Internet at http://pubs.acs.org.

■ AUTHOR INFORMATION

Corresponding Author

konrad.koszinowski@cup.uni-muenchen.de

■ ACKNOWLEDGMENTS

We thank Prof. Herbert Mayr for his continuous generous support and gratefully acknowledge financial support from LMU München (LMUexcellent), Deutsche Forschungsgemeinschaft (SFB 749), the Center for Integrated Protein Science Munich, the Fonds der Chemischen Industrie, and the Dr. Otto Röhm Gedächtnisstiftung.

■ REFERENCES

(1) *The Chemistry of Organocopper Compounds*; Rappoport, Z., Marek, I., Eds.; Wiley: Hoboken, NJ, 2009.

(2) For the few cases of known stable organocopper(II) species, see: Van Koten, G.; Jastrzebski, J. T. B. H. In *The Chemistry of Organocopper Compounds*; Rappoport, Z., Marek, I., Eds.; Wiley: Hoboken, NJ, 2009; pp 23−143.
(3) For the very few cases of reported stable organocopper(III) species, see: (a) Willert-Porada, M. A.; Burton, D. J.; Baenziger, N. C. *J. Chem. Soc., Chem. Commun.* **1989**, 1633−1634. (b) Naumann, D.; Roy, T.; Tebbe, K.-F.; Crump, W. *Angew. Chem.* **1993**, *105*, 1555−1556; *Angew. Chem., Int. Ed. Engl.* **1993**, *32*, 1482−1483.
(4) (a) Whitesides, G. M.; Fischer, W. F. Jr.; San Filippo, J. Jr.; Bashe, R. W.; House, H. O. *J. Am. Chem. Soc.* **1969**, *97*, 4871−4882. (b) Vermeer, P.; Meijer, J.; Brandsma, L. *Recl. Trav. Chim.* **1975**, *94*, 112−114. (c) Luche, J. L.; Barreiro, E.; Dollat, J. M.; Crabbe, P. *Tetrahedron Lett.* **1975**, *16*, 4615−4618. (d) Goering, H. L.; Kantner, S. S. *J. Org. Chem.* **1983**, *48*, 721−724.
(5) (a) Nakamura, E.; Mori, S.; Morokuma, K. *J. Am. Chem. Soc.* **1997**, *119*, 4900−4910. (b) Mori, S.; Nakamura, E. *Chem.—Eur. J.* **1999**, *5*, 1534−1543. (c) Nakamura, E.; Yamanaka, M. *J. Am. Chem. Soc.* **1999**, *121*, 8941−8942. (d) Nakamura, E.; Mori, S. *Angew. Chem.* **2000**, *112*, 3902−3924; *Angew. Chem., Int. Ed.* **2000**, *39*, 3750−3771.
(6) Snyder, J. P. *Angew. Chem.* **1995**, *107*, 112−113; *Angew. Chem., Int. Ed. Engl.* **1995**, *34*, 80−81.
(7) (a) Bertz, S. H.; Cope, S.; Murphy, M.; Ogle, C. A.; Taylor, B. J. *J. Am. Chem. Soc.* **2007**, *129*, 7208−7209. (b) Bertz, S. H.; Cope, S.; Dorton, D.; Murphy, M.; Ogle, C. A. *Angew. Chem.* **2007**, *119*, 7212−7215; *Angew. Chem., Int. Ed.* **2007**, *46*, 7082−7085. (c) Bartholomew, E. R.; Bertz, S. H.; Cope, S.; Dorton, D. C.; Murphy, M.; Ogle, C. A. *Chem. Commun.* **2008**, 1176−1177. (d) Bartholomew, E. R.; Bertz, S. H.; Cope, S.; Murphy, M.; Ogle, C. A. *J. Am. Chem. Soc.* **2008**, *130*, 11244−11245. (e) Bartholomew, E. R.; Bertz, S. H.; Cope, S. K.; Murphy, M. D.; Ogle, C. A.; Thomas, A. A. *Chem. Commun.* **2010**, *46*, 1253−1254. (f) Bertz, S. H.; Murphy, M. D.; Ogle, C. A.; Thomas, A. A. *Chem. Commun.* **2010**, *46*, 1255−1256. (g) Bertz, S. H.; Moazami, Y.; Murphy, M. D.; Ogle, C. A.; Richter, J. D.; Thomas, A. A. *J. Am. Chem. Soc.* **2010**, *132*, 9549−9551.
(8) (a) Gärtner, T.; Henze, W.; Gschwind, R. M. *J. Am. Chem. Soc.* **2007**, *129*, 11362−11363. (b) Henze, W.; Gärtner, T.; Gschwind, R. M. *J. Am. Chem. Soc.* **2008**, *130*, 13718−13726. (c) Gärtner, T.; Yoshikai, N.; Neumeier, M.; Nakamura, E.; Gschwind, R. M. *Chem. Commun.* **2010**, *46*, 4625−4626.
(9) (a) Yamashita, M.; Fenn, J. B. *J. Phys. Chem.* **1984**, *88*, 4451−4459. (b) Yamashita, M.; Fenn, J. B. *J. Phys. Chem.* **1984**, *88*, 4671−4675.
(10) For selected reviews and highlights, see: (a) Plattner, D. A. *Int. J. Mass Spectrom.* **2001**, *207*, 125−144. (b) Chen, P. *Angew. Chem.* **2003**, *115*, 2938−2954; *Angew. Chem., Int. Ed.* **2003**, *42*, 2832−2847. (c) Henderson, W.; McIndoe, J. S. *Mass Spectrometry of Inorganic, Coordination and Organometallic Compounds: Tools, Techniques, Tips*; Wiley: Chichester, 2005; pp 175−219. (d) Müller, C. A.; Markert, C.; Teichert, A. M.; Pfaltz, A. *Chem. Commun.* **2009**, 1607−1618. (e) Agrawal, D.; Schröder, D. *Organometallics* **2011**, *30*, 32−35. (f) Coelho, F.; Eberlin, M. N. *Angew. Chem.* **2011**, *123*, 5370−5372; *Angew. Chem., Int. Ed.* **2011**, *50*, 5261−5263.
(11) (a) Lipshutz, B. H.; Stevens, K. L.; James, B.; Pavlovich, J. G.; Snyder, J. P. *J. Am. Chem. Soc.* **1996**, *118*, 6796−6797. (b) Lipshutz, B. H.; Keith, J.; Buzard, D. J. *Organometallics* **1999**, *18*, 1571−1574.
(12) (a) Putau, A.; Koszinowski, K. *Organometallics* **2010**, *29*, 3593−3601; **2010**, *29*, 6841−6842, (Addition/Correction). (b) Putau, A.; Koszinowski, K. *Organometallics* **2011**, *30*, 4771−4778.
(13) (a) James, P. F.; O'Hair, R. A. J. *Org. Lett.* **2004**, *6*, 2761−2764. (b) Rijs, N.; Khairallah, G. N.; Waters, T.; O'Hair, R. A. J. *J. Am. Chem. Soc.* **2008**, *130*, 1069−1079. (c) Rijs, N. J.; Yates, B. F.; O'Hair, R. A. J. *Chem.—Eur. J.* **2010**, *16*, 2674−2678. (d) Rijs, N. R.; O'Hair, R. A. J. *Organometallics* **2010**, *29*, 2282−2291.
(14) Lipton, M. F.; Sorensen, C. M.; Sadler, A. C.; Shapiro, R. H. *J. Organomet. Chem.* **1980**, *186*, 155−158.
(15) (a) Uchiyama, M.; Furuyama, T.; Kobayashi, M.; Matsumoto, Y.; Tanaka, K. *J. Am. Chem. Soc.* **2006**, *128*, 8404−8405. (b) Koszinowski, K.; Böhrer, P. *Organometallics* **2009**, *28*, 100−110. (c) Hunter, H. N.; Hadei, N.; Blagojevic, V.; Patschinski, P.; Achonduh, G. T.; Avola, S.; Bohme, D. K.; Organ, M. G. *Chem.—Eur. J.* **2011**, *17*, 7845−7851.
(16) (a) Satterfield, M.; Brodbelt, J. S. *Inorg. Chem.* **2001**, *40*, 5393−5400. (b) Zins, E.-L.; Pepe, C.; Schröder, D. *J. Mass Spectrom.* **2010**, *45*, 1253−1260.
(17) Gabelica, V.; De Pauw, E. *Mass Spectrom. Rev.* **2005**, *24*, 566−587.
(18) Carvajal, C.; Tölle, K. J.; Smid, J.; Szwarc, M. *J. Am. Chem. Soc.* **1965**, *87*, 5548−5553.
(19) Krasovskiy, A.; Knochel, P. *Synthesis* **2006**, 890−891.
(20) Frisch, M. J.; et al. *Gaussian 03*, Revision D.01; Gaussian, Inc.: Wallingford, CT, 2004.
(21) Hu, H.; Snyder, J. P. *J. Am. Chem. Soc.* **2007**, *129*, 7210−7211.
(22) Becke, A. D. *J. Chem. Phys.* **1993**, *98*, 5648−5652.
(23) Leininger, T.; Nicklass, A.; Stoll, H.; Dolg, M.; Schwerdtfeger, P. *J. Chem. Phys.* **1996**, *105*, 1052−1059.
(24) Rassolov, V. A.; Pople, J. A.; Ratner, M. A.; Windus, T. L. *J. Chem. Phys.* **1998**, *109*, 1223−1229.
(25) Figgen, D.; Rauhut, G.; Dolg, M.; Stoll, H. *Chem. Phys.* **2005**, *311*, 227−244.
(26) Møller, C.; Plesset, M. S. *Phys. Rev.* **1934**, *46*, 618−622.
(27) Perdew, J. P.; Burke, K.; Wang, Y. *Phys. Rev. B* **1996**, *54*, 16533−16539.
(28) Adamo, C.; Barone, V. *J. Chem. Phys.* **1998**, *108*, 664−675.
(29) Glendening, E. D.; Reed, A. E.; Carpenter, J. E.; Weinhold, F. *NBO*, Version 3.1; University of Wisconsin: Madison, WI, 1993.
(30) Ingold, C. K. *Structure and Mechanism in Organic Chemistry*, 2nd ed.; Cornell University Press: Ithaca, NY, 1969; pp 428−448.
(31) Kondo, Y.; Matsudaira, T.; Sato, J.; Murata, N.; Sakamoto, T. *Angew. Chem.* **1996**, *108*, 818−820; *Angew. Chem., Int. Ed. Engl.* **1996**, *35*, 736−738.
(32) (a) Langham, W.; Brewster, R. Q.; Gilman, H. *J. Am. Chem. Soc.* **1941**, *63*, 545−549. (b) Bailey, W. F.; Patricia, J. J. *J. Organomet. Chem.* **1988**, *352*, 1−46. (c) Krasovskiy, A.; Straub, B. F.; Knochel, P. *Angew. Chem.* **2006**, *118*, 165−169; *Angew. Chem., Int. Ed.* **2006**, *45*, 5974−5978.
(33) (a) Moret, M.-E.; Serra, D.; Bach, A.; Chen, P. *Angew. Chem.* **2010**, *122*, 2935−2939; *Angew. Chem., Int. Ed.* **2010**, *49*, 2873−2877. (b) Serra, D.; Moret, M.-E.; Chen, P. *J. Am. Chem. Soc.* **2011**, *133*, 8914−8926.
(34) Fuoss, R. M.; Kraus, C. A. *J. Am. Chem. Soc.* **1933**, *55*, 2387−2399.
(35) (a) Koszinowski, K. *J. Am. Chem. Soc.* **2010**, *132*, 6032−6040. (b) Schröder, D.; Ducháčková, L.; Tarábek, J.; Karwowska, M.; Fijalkowski, K. J.; Ončák, M.; Slavíček, P. *J. Am. Chem. Soc.* **2011**, *133*, 2444−2451. (c) Fleckenstein, J. E.; Koszinowski, K. *Organometallics* **2011**, *30*, 5018−5026.
(36) (a) Iribarne, J. V.; Thomson, B. A. *J. Chem. Phys.* **1976**, *64*, 2287−2294. (b) Thomson, B. A.; Iribarne, J. V. *J. Chem. Phys.* **1979**, *71*, 4451−4463.
(37) (a) Wang, H.; Agnes, G. R. *Anal. Chem.* **1999**, *71*, 3785−3792. (b) Wang, H.; Agnes, G. R. *Anal. Chem.* **1999**, *71*, 4166−4172. (c) Wortmann, A.; Kistler-Momotova, A.; Zenobi, R.; Heine, M. C.; Wilhelm, O.; Pratsinis, S. E. *J. Am. Soc. Mass Spectrom.* **2007**, *18*, 385−393. (d) Tsierkezos, N. G.; Roithová, J.; Schröder, D.; Ončák, M.; Slavíček, P. *Inorg. Chem.* **2009**, *48*, 6287−6296.
(38) Luedtke, W. D.; Landman, U.; Chiu, Y.-H.; Levandier, D. J.; Dressler, R. A.; Sok, S.; Gordon, M. S. *J. Phys. Chem. A* **2008**, *112*, 9628−9649.
(39) Karlström, A. S. E.; Bäckvall, J.-E. *Chem.—Eur. J.* **2001**, *7*, 1981−1989.
(40) Norinder, J.; Bäckvall, J.-E.; Yoshikai, N.; Nakamura, E. *Organometallics* **2006**, *25*, 2129−2132.
(41) Mori, S.; Nakamura, E.; Morokuma, K. *J. Am. Chem. Soc.* **2000**, *122*, 7294−7307.
(42) Yamanaka, M.; Kato, S.; Nakamura, E. *J. Am. Chem. Soc.* **2004**, *126*, 6287−6293.
(43) Pratt, L. M.; Voit, S.; Mai, B. K.; Nguyen, B. H. *J. Phys. Chem. A* **2010**, *114*, 5005−5015.